Received: 18 November 2021 | Accepted: 25 April 2022

DOI: 10.1002/jcp.30775

RESEARCH ARTICLE

Journal of Cellular Physiology WILEY

Modulation of I_{Ks} channel–PIP_2 interaction by PRMT1 plays a critical role in the control of cardiac repolarization

Xue An[1] | Jiwon Lee[2] | Ga Hye Kim[2] | Hyun-Ji Kim[1] | Hyun-Jeong Pyo[1] | Ilmin Kwon[2] | Hana Cho[1]

[1]Department of Physiology, Sungkyunkwan University School of Medicine, Suwon, Korea

[2]Department of Anatomy and Cell Biology, Sungkyunkwan University School of Medicine, Suwon, Korea

Correspondence

Ilmin Kwon, Department of Anatomy and Cell Biology, Sungkyunkwan University School of Medicine, Suwon 16419, Korea.
Email: ilmin.kwon@skku.edu

Hana Cho, Department of Physiology, Sungkyunkwan University School of Medicine, Suwon 16419, Korea.
Email: hanacho@skku.edu

Funding information

National Research Foundation of Korea, Grant/Award Numbers: NRF-2019R1A2C2003767, NRF-2020R1A2C2012846

Abstract

Recent studies have shown that protein arginine methyltransferase 1 (PRMT1) is highly expressed in the human heart, and loss of PRMT1 contributes to cardiac remodeling in the heart failure. However, the functional importance of PRMT1 in cardiac ion channels remains uncertain. The slow activating delayed rectifier K^+ (I_{Ks}) channel is a cardiac K^+ channel composed of KCNQ1 and KCNE1 subunits and is a new therapeutic target for treating lethal arrhythmias in many cardiac pathologies, especially heart failure. Here, we demonstrate that PRMT1 is a critical regulator of the I_{Ks} channel and cardiac rhythm. In the guinea pig ventricular myocytes, treatment with furamidine, a PRMT1-specific inhibitor, prolonged the action potential duration (APD). We further show that this APD prolongation was attributable to I_{Ks} reduction. In HEK293T cells expressing human KCNQ1 and KCNE1, inhibiting PRMT1 via furamidine reduced I_{Ks} and concurrently decreased the arginine methylation of KCNQ1, a pore-forming α-subunit. Evidence presented here indicates that furamidine decreased I_{Ks} mainly by lowering the affinity of I_{Ks} channels for the membrane phospholipid, phosphatidylinositol 4,5-bisphosphate (PIP_2), which is crucial for pore opening. Finally, applying exogenous PIP_2 to cardiomyocytes prevented the furamidine-induced I_{Ks} reduction and APD prolongation. Taken together, these results indicate that PRMT1 positively regulated I_{Ks} activity through channel–PIP_2 interaction, thereby restricting excessive cardiac action potential.

KEYWORDS

arrhythmia, cardiac myocytes, delayed rectifier potassium channel, PIP_2, PRMT1

1 | INTRODUCTION

Protein methylation has been known to control various cellular functions by regulating signaling pathways and/or gene expression (Bedford & Clarke, 2009; Biggar & Li, 2015). Protein arginine methyltransferases (PRMTs) catalyze the transfer of a methyl group to arginine residues of their target proteins (Bedford & Richard, 2005). In mammals, nine PRMTs have been characterized, and PRMT1, originally identified as a histone H4 methyltransferase, methylates several nonhistone proteins and is implicated in diverse cellular processes, including hepatic gluconeogenesis and skeletal muscle function (Blanc et al., 2017; D. Choi et al., 2012; Di Lorenzo &

Bedford, 2011; S. Huang et al., 2005). Recent reports have demonstrated the role of PRMT1 signaling in the pathogenesis of cardiac hypertrophy and heart failure. Albrecht et al. (2015) showed that desmoplakin is a target of PRMT1, and its methylation deficiency is associated with cardiomyopathy. Another study reported that PRMT1 knockout impaired alternative messenger RNA splicing in the heart (Murata et al., 2018). It was also reported that the hearts of patients experiencing heart failure exhibited reduced PRMT1 levels, and cardiac-specific PRMT1 ablation caused heart failure in mice (Pyun et al., 2018). However, the role of PRMT1 in controlling the function of cardiac ion channels remains unclear.

The slow delayed rectifier potassium current (I_{Ks}) is the slow component of the cardiac delayed rectifier potassium current and is critical for late-phase repolarization of cardiac action potential (AP). Pore-forming KCNQ1 α-subunits coassemble with accessory KCNE1 β-subunits to form I_{Ks} channels, and mutations in any subunit can induce severe long QT syndrome (LQT-1, LQT-5) as characterized by delayed ventricular repolarization, syncope, and sudden death (Liu et al., 2012). Because I_{Ks} plays a key role in regulating AP repolarization and is important in maintaining normal heart rhythms, loss of this current is highly arrhythmogenic (Shugg et al., 2020). Animal models of heart failure and cardiomyocytes isolated from failing hearts consistently demonstrate reduced I_{Ks} and prolonged cardiac action potential duration (APD), which contribute to fatal ventricular arrhythmias. Therefore, recently, the I_{Ks} channel is expected to be a promising target for antiarrhythmic drugs. However, unfortunately, ion-channel-modulating drugs have not yet yielded a satisfactory outcome due to a lack of channel or tissue selectivity, or poor bioavailability (Cardiac Arrhythmia Suppression Trial Investigators, 1989; Schumacher & Martens, 2010; Waldo et al., 1996). Thus, molecular pathways and mechanisms that modulate I_{Ks} activities should be defined to develop new and improved therapies.

I_{Ks} channels are activated by membrane depolarization, but their activation also requires the membrane lipid, phosphatidylinositol 4,5-bisphosphate (PIP_2) (Sun & MacKinnon, 2020). PIP_2 binds to KCNQ1 and likely acts to stabilize the channel in an open state (Sun & MacKinnon, 2020). Hence, I_{Ks} activities can be regulated by the PIP_2 availability or the modulation of the PIP_2 affinity of I_{Ks}. G protein-coupled receptors (GPCRs), which signal through different heterotrimeric G-protein subtypes ($G_{q/11}$, G_s, $G_{i/o}$, and $G_{12/13}$) to an array of downstream signaling cascades, are key elements in the repertoire of extracellular signal-regulated receptors in cardiac myocytes with relevance to PIP_2 regulatory dynamics. Among GPCR signaling, β-adrenergic stimulation can markedly enhance I_{Ks} (Shugg et al., 2020) through a mechanism involving modulation of the PIP_2 affinity of I_{Ks} (Lo & Numann, 1998; Matavel et al., 2010). Activation of β-adrenergic receptors stimulates adenylyl cyclase, which catalyzes the conversion of ATP to cAMP, then activates protein kinase A (PKA). PKA immediately phosphorylates KCNQ1, resulting in an increased affinity of I_{Ks} for PIP_2 (Lo & Numann, 1998; Matavel et al., 2010). On the other hand, the PIP_2 availability is regulated by stimulation of a $G_{q/11}$ protein-coupled receptor, whereby activated phospholipase Cβ hydrolyzes PIP_2 into soluble inositol 1,4,5-trisphosphate and membrane-bound diacylglycerol (Delmas & Brown, 2005). Acute activation of α1-adrenergic receptors has been demonstrated to reduce I_{Ks} through a cellular depletion of PIP_2 (Kienitz et al., 2016; Tobelaim et al., 2017). However, it remains unknown whether other major signaling pathways that have significant effects on cardiac myocytes, modulate PIP_2 regulation of I_{Ks}.

Previous studies have shown that PRMT1-mediated arginine methylation facilitates neuronal KCNQ2 channel–PIP_2 interaction; thus, PRMT1 catalysis may be a general mechanism for regulating ion flux physiology (Kim et al., 2016). Here, we investigated whether PRMT1 signaling regulates the I_{Ks} channel and cardiac rhythm. To overcome the paucity of I_{Ks} in adult mouse hearts, we used cardiomyocytes from adult guinea pigs, which express native I_{Ks}. In guinea pig ventricular myocytes, we observed that the conductance-voltage relationship of native cardiac I_{Ks} was subject to tonic regulation by the PRMT1 pathway, and PRMT1 inhibition prolonged ventricular APD by reducing I_{Ks}. Reconstituting the I_{Ks} channels in HEK293T cells with human KCNQ1 and KCNE1 subunits revealed that PRMT1 inhibition-induced I_{Ks} reduction was correlated with reduced KCNQ1 methylation levels, and PRMT1 function is essential for the channel to bind to PIP_2. Consistently, adding exogenous PIP_2 to cardiomyocytes prevented furamidine-induced I_{Ks} reduction and APD prolongation. These data demonstrate a PRMT1-mediated modulation of cardiac I_{Ks} activity that may be a key target for preventing excessive APD prolongation and arrhythmias in patients with heart failure.

2 | MATERIALS AND METHODS

2.1 | Guinea pig ventricular myocyte isolation and recording

Ventricular cells were isolated from the hearts of guinea pigs weighing 200–250 g using enzymatic dissociation as previously described (S. H. Choi et al., 2014). All experimental procedures were conducted in accordance with the guidelines of the Sungkyunkwan University School of Medicine Institutional Animal Care and Use Committee (approval no. SKKUIACUC2019-07-11-3). Briefly, guinea pigs were injected with heparin (1.0 units/kg) and euthanized by stunning/induced coma with loss of all reflex responses, followed by cardiac excision. The heart was cannulated using an 18-Gauge needle, then retrogradely perfused via the aorta on a Langendorff apparatus. During coronary perfusion, all perfusates were maintained at 37°C and equilibrated with 100% O_2. The hearts were initially perfused with normal Tyrode solution for 2–3 min to clear the blood, then perfused with Ca^{2+}-free solution for 2 min. Finally, the hearts were perfused with enzyme solution containing 1 mg/ml collagenase (Worthington Type 2) and 0.1 mg/ml protease (Sigma-Aldrich) in Ca^{2+}-free solution for 14–16 min, then the ventricles were separated from the atria and cut into small pieces. Single cells were dissociated in high K^+/low Cl^- solution from these small pieces using a blunt-tip glass pipette and stored in the same solution at 4°C until use.

We used the conventional whole-cell patch-clamp technique to record membrane currents or voltages from single isolated myocytes using an EPC-10 amplifier (HEKA Instrument). In current-clamp mode, APs were evoked by a brief suprathreshold current pulse. In voltage-clamp mode, access resistance was monitored through the experiments, and data were accepted only when access resistance was kept at <10 MΩ. Filtered signals (10 kHz) from a patch-clamp amplifier (EPC-10; HEKA Instrument) were digitized at 20 kHz and stored on a personal computer for later analysis. The patch pipettes (World Precision Instruments) were made by a Narishige puller (PP-830; Narishige) and had a resistance of 3 ± 0.5 MΩ when filled with the pipette solution. All electrophysiological experiments were performed at 34–35°C. The bath solution (or normal Tyrode solution) contained (mM): 143 NaCl, 5.4 KCl, 5 HEPES, 0.5 NaH_2PO_4, 11.1 glucose, 0.5 $MgCl_2$, and 1.8 $CaCl_2$, at pH 7.4 adjusted with NaOH. The pipette solution for perforated patches contained (mM): 140 KCl, 10 HEPES, 1 $MgCl_2$, and 5 EGTA, titrated to pH 7.2 with KOH. APs were recorded using a nystatin-perforated patch-clamp configuration, with an EPC10 patch-clamp amplifier (HEKA Instrument). Data were digitized, and the current injections (125–175 pA, 9 ms) for AP generation were controlled using Patchmaster software. For voltage-clamp experiments to analyze I_{Ks}, standard whole-cell voltage-clamp techniques were used. The pipette solution for I_{Ks} contained (in mM): 110 KCl, 1 $MgCl_2$, 5 K_2-ATP, 10 EGTA, 10 HEPES, pH 7.4 adjusted with KOH. Na^+ current was inactivated by holding at −50 mV; Ca^{2+} current was inhibited by the addition of 1 μM isradipine to the external solution.

The voltage dependence of the current activation was estimated by tail current analysis. The tail current amplitude was plotted as a function of the test potential (V_t) and the data for individual cells fitted with a Boltzmann function: $I = I_{max}/[1 + \exp[(V_t - V_{0.5})/k]]$, where I_{max} is the maximal current, V_t is the test potential, $V_{0.5}$ is the membrane potential at which 50% of the channels are activated, and k is the slope factor. Current densities (pA/pF) were obtained after being normalized to the cell surface area calculated by Patchmaster.

2.2 | HEK293T cell electrophysiology

The HEK293T cells were grown in Dulbecco's modified Eagle's medium (Gibco; Thermo Fisher Scientific) supplemented with 10% fetal bovine serum (Gibco; Thermo Fisher Scientific), 100 IU/ml penicillin, and 100 μg/ml streptomycin at 37°C in an incubator in a humidified atmosphere of 5% CO_2/95% air. For transient transfections, 1.1 μg of KCNQ1 and 0.4 μg of KCNE1 subunits linked to a green fluorescent protein(GFP) were cotransfected using Effectene (Qiagen) according to the manufacturer's protocol. At between 24 and 30 h upon transfection, cells were subjected to electrophysiological analysis. For expression of voltage-sensitive phosphatase from *Danio rerio* (Dr-VSP), 0.4 μg of Dr-VSP DNA was coexpressed. The transfection efficiency was ~65%.

I_{Ks} activities were measured using the whole-cell patch-clamp technique as previously described (Ki et al., 2014). Voltage clamping was performed using an EPC-10 amplifier (HEKA Instrument) and filtered at 10 kHz. The patch pipettes (World Precision Instruments) were made by a Narishige puller (PP-830; Narishige) and had a resistance of 2–3 MΩ when filled with the pipette solutions listed below. All recordings were taken at room temperature. The normal external solution for HEK293 cell recording contained (in mM) 143 NaCl, 5.4 KCl, 5 HEPES, 0.5 NaH_2PO_4, 11.1 glucose, 0.5 $MgCl_2$, and 1.8 $CaCl_2$, at pH 7.4 adjusted with NaOH. The pipette solution contained (in mM) 135 K^+ aspartate, 2 $MgCl_2$, 3 EGTA, 1 $CaCl_2$, 4 Mg-ATP, 0.1 Na-GTP, and 10 HEPES, at pH 7.4 adjusted with KOH. Currents were analyzed and fitted using Patchmaster (HEKA Instrument) and Origin 6.1 (Originlab Corp) software. All values are given as means ± SEM.

2.3 | Immunoprecipitation and Western blotting

HEK293T cells were transfected with 4 μg of Flag-tagged KCNQ1 (Flag-KCNQ1) and 4 μg of GFP-tagged KCNE1 (GFP-KCNE1) using Lipofectamine 2000 (Thermo Fisher Scientific) according to the manufacturer's protocol. At 48 h after transfection, cells were incubated with 20 μM of furamidine for 5 h. The cells were then collected in immunoprecipitation buffer (50 mM Tris-HCl pH 8.0, 150 mM NaCl, 1% Triton X-100, 1 mM ethylenediaminetetraacetic acid, and protease inhibitor) and lysed by sonication twice for 10 s (2 s on/10 s off ice) at 3% power. Upon clearance by centrifugation at 15,000 rpm for 15 min at 4°C, the lysates were incubated with anti-Flag antibody (Sigma-Aldrich) with gentle rotation overnight at 4°C. The immune complexes were then supplemented with protein G magnetic beads (Bio-Rad) for 2 h at 4°C. The samples were then washed three times with ice-cold phosphate-buffered saline. The bound proteins were eluted using a 2X sodium dodecyl sulfate sample buffer by boiling at 95°C for 10 min. For Western blotting, the samples were separated using NuPAGE 4–12% Bis-Tris Gel (Thermo Fisher Scientific) and then transferred onto the nitrocellulose membrane (Bio-Rad). The samples were detected using anti-Flag, anti-monomethyl arginine (Cell Signaling Technology), and anti-dimethyl arginine, asymmetric (Merck) antibodies.

2.4 | Chemicals

Chromanol 293B and TP-064 were purchased from Tocris Bioscience (Bristol); DiC8-PIP_2 was from Echelon Biosciences; and GSK3368715 was purchased from Selleck Chemicals. All other drugs and chemicals were purchased from Sigma-Aldrich.

2.5 | Statistics

Data were analyzed with Origin (Version 6.1; OriginLab). All results are presented as the mean ± SEM with the number of cells (n) used in each experiment. Statistical significance was evaluated using

Student's *t*-test and the level of significance was indicated by the number of marks. $p > 0.05$ was regarded as not significantly different (NS).

3 | RESULTS

3.1 | PRMT1 inhibition prolonged APD in guinea pig ventricular myocytes via I_{Ks}

First, we investigated whether PRMT1 inhibition could modulate membrane excitability of cardiac myocytes using guinea pig ventricular myocytes. APs were elicited in the current-clamp mode by applying depolarizing current pulses at various stimulation frequencies. Inhibiting PRMT1 function with 20 μM furamidine (Kim et al., 2016) significantly prolonged APD (Figure 1a). Furamidine treatment significantly increased the time required for 90% repolarization (APD_{90}) at all stimulation rates (cycle length [CL]: 0.5, 1, 2, and 4 s; Figure 1b). Neither the resting membrane potential (RMP) nor the AP overshoot potentials changed during furamidine treatment. The mean RMP and overshoot potentials after furamidine treatment were −81.1 ± 0.23 mV ($n = 7$; ns vs. −81.0 ± 0.19 mV in the absence of furamidine) and −45.2 ± 0.11 mV ($n = 7$; ns vs. −48.22 ± 0.35 mV in the absence of furamidine), respectively.

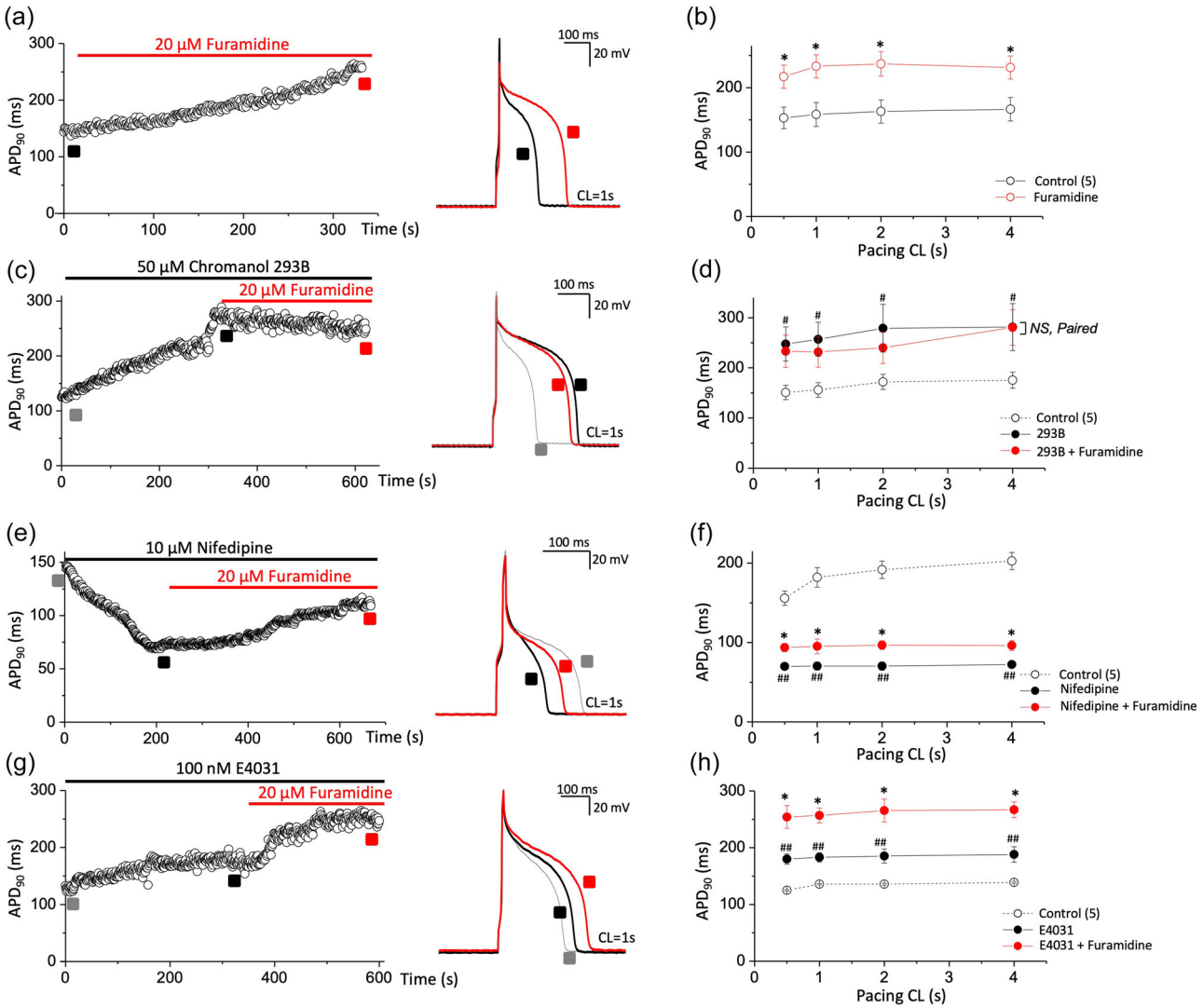

FIGURE 1 PRMT1 inhibition with furamidine, a PRMT1 specific inhibitor, prolongs action potential duration (APD) in guinea pig ventricular myocytes via I_{Ks} activity. (a,c,e,g) Action potentials (APs) were elicited consecutively at a pacing cycle length (CL) of 1 s and values of APD at 90% repolarization (APD_{90}) were plotted over time. APD_{90} was consecutively recorded during furamidine application from a cell in control (a) or after pretreatment with chromanol 293B (c), nifedipine (e), or E4031 (g). Right, representative AP traces before (black in each panel) and after furamidine (red in each panel) treatment. AP traces before channel blocker application were also superimposed (gray in c, e, and g panels). (b,d,f,h) The summary data for the APD_{90} during stimulation at various pacing CLs. NS, not significantly different; $^{*}p < 0.05$ control or channel blocker versus furamidine treatment; paired Student's *t*-test. $^{\#}p < 0.05$, $^{\#\#}p < 0.01$ control versus each channel blocker in the same group; paired Student's *t*-test. All data are mean ± SEM. PRMT1, protein arginine methyltransferase 1.

APD prolongation of cardiomyocytes typically results from reducing the rapid component (I_{Kr}) of delayed rectifier current (I_K) and the slower component (I_{Ks}) or from increasing the$_L$-type Ca^{2+} currents (LTCC). To examine the ionic mechanism(s) underlying APD prolongation in the furamidine-treated ventricular myocytes, we first used chromanol 293B, an I_{Ks} blocker. Consistent with the previous study (Bosch et al., 1998), 50 μM chromanol 293B prolonged APD_{90}. In the presence of chromanol 293B, 20 μM furamidine did not further prolong the APD (Figure 1c,d). We also examined the effects of E4031, an I_{Kr} blocker, and nifedipine, an LTCC blocker. Nifedipine reduced the APD, and E4031 prolonged the APD, but neither blocked the effects of furamidine in the guinea pig ventricular myocytes (Figure 1e–h). These data imply that PRMT1 regulates cardiac AP mainly via I_{Ks}.

3.2 | PRMT1 inhibition reduced I_{Ks} activity in guinea pig ventricular myocytes

Because the I_{Ks}-specific inhibitor blocked the effect of furamidine, we next investigated whether furamidine could specifically regulate I_{Ks} in cardiac myocytes. We recorded the I_{Ks} in guinea pig ventricular myocytes in voltage-clamp mode by using the recording protocol to isolate I_{Ks} as previously reported (Nuss & Marban, 1994; Wang et al., 2011). Briefly, a holding potential of −50 mV was used to inactivate the voltage-gated Na^+ channels, and 1 μM isradipine was included in the bath solution to block voltage-gated Ca^{2+} channel currents. Native I_{Ks} was defined as the difference in the isolated current by subtracting the current measured in the presence of 50 μM chromanol 293B from the current measured before administering the drug (Wang et al., 2011). Currents were evoked via 2-s test pulses from −30 to +70 mV in 20-mV increments, followed by 3-s tail current pulses to −30 mV and 15-s interpulse intervals. Consistent with the previous study (Wang et al., 2011), chromanol 293B-sensitive, time-dependent, slow activating delayed rectifier currents developed during depolarization, and the outward tail current deactivated during repolarization (Figure 2a). As indicated by the representative data before and after 20 μM furamidine treatment, furamidine significantly decreased the I_{Ks} current. The diary plot in Figure 2b illustrates the time course of the decreased tail current. The average furamidine-mediated decrease in the tail current amplitude at +70 mV was 57.1 ± 0.2% (n = 5, Figure 2c). As indicated by the current records obtained during the furamidine treatment and mean I–V relationships, furamidine decreased the I_{Ks} without changing the shape of the I–V relationships. Furamidine treatment did not alter the activation curve, and the mean $V_{1/2}$ value after furamidine treatment was 11.62 ± 0.12 mV (n = 5; ns vs. 8.23 ± 1.45 mV in the absence of furamidine; Figure 2d). These findings indicate that furamidine reduced the I_{Ks} activity in guinea pig ventricular myocytes.

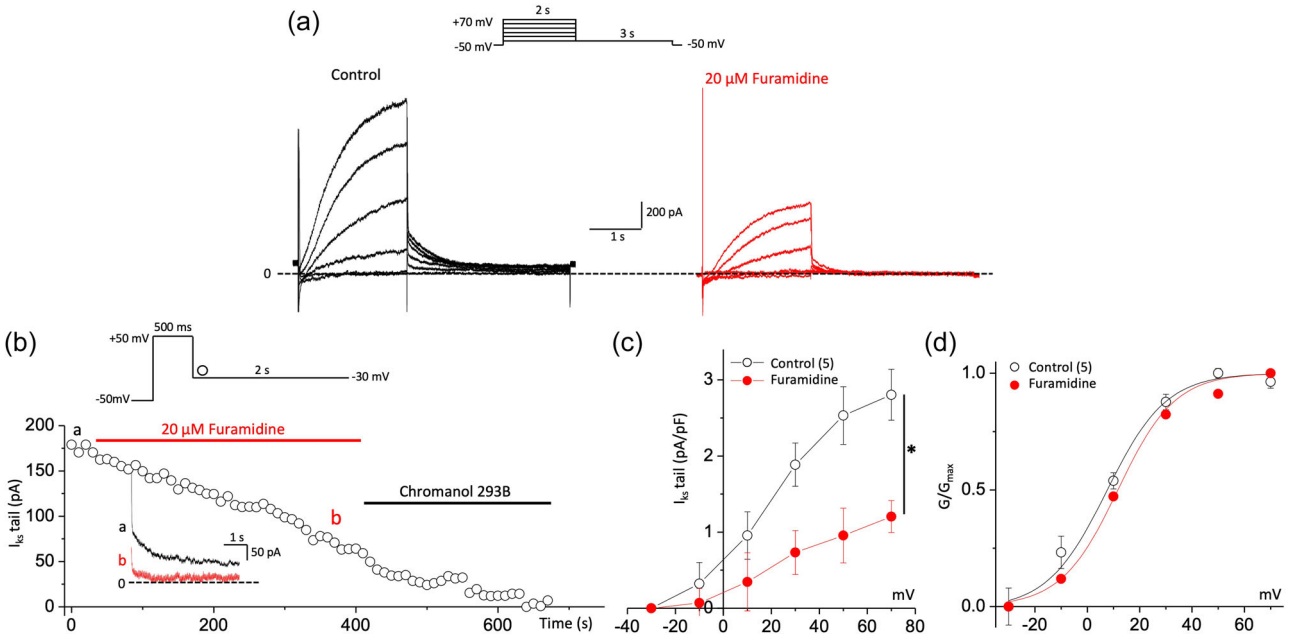

FIGURE 2 PRMT1 inhibition reduces I_{Ks} activity in guinea pig ventricular myocytes. (a) Representative current trace of I_{Ks} before (black) and after 20 μM furamidine treatment (red) in ventricular myocytes of guinea pig. *Inset* shows the pulse protocol. (b) Time course of change in the amplitude of the I_{Ks} tail (deactivation) during applications of furamidine. Representative current traces obtained at the points indicated by (a) and (b) are also shown on an expanded time scale in the inset. Currents were elicited by a voltage step to +50 mV at a holding potential of −50 mV with a subsequent step to −30 mV for the tail current. (c) The current–voltage (I–V) relationships were obtained before and after the application of furamidine. Currents were elicited by voltage steps from −30 to +70 mV with a subsequent step to −30 mV for the tail current. (d) Steady-state activation curves, with relative conductance derived from maximal chord conductance and reversal potential (E_{rev}) for each I–V, and peak $I_K/(E_m - E_{rev})$. The resulting conductance was normalized to the maximal chord conductance. Data were fitted to a Boltzmann function (*smooth curves*). *p < 0.05 by paired Student's t-test. All data are mean ± SEM. PRMT1, protein arginine methyltransferase 1.

3.3 | PRMT1 methylated the KCNQ1 subunits of I_{Ks} channels

Because PRMTs can mediate ion channel activities/functions by methylating channel proteins (Kim et al., 2016; Lee et al., 2019), we hypothesized that PRMT1 regulation of I_{Ks} would result from directly modifying the channel. To test this, we first reconstituted the channel by expressing human clone KCNQ1 and KCNE1 subunits in HEK293T cells, which recapitulated the regulatory behaviors in the guinea pig ventricular myocytes. Cotransfection of wild-type KCNQ1 and KCNE1 produced the slowly activating and deactivating, voltage-dependent current, I_{Ks} (Figure 3a, left). Furamidine treatment (20 μM, 5 min) markedly decreased the human I_{Ks} in HEK293T cells (Figure 3a, right) without noticeably altering the shape of the *I–V* relationships or $V_{1/2}$ (Figure 3b,c), which was consistent with the changed current density observed in the native cells (Figure 2). We further validated the effects of PRMT1 inhibition on I_{Ks} activity with the type I PRMT inhibitor GSK3368715 which shows more efficacy towards PRMT1, PRMT6, and PRMT8 (Eram et al., 2016; Fedoriw et al., 2019). Similar to furamidine, the treatment of GSK3368715 significantly decreased I_{Ks} activity without altering the shape of the *I–V* relationships or $V_{1/2}$ in HEK293T cells (Supporting Information: Figure 1a–c). In contrast to furamidine and GSK3368715, TP-064, a potent and selective inhibitor of PRMT4 (Zhang et al., 2021) had no significant effect on I_{Ks} activity in HEK293T cells (Supporting Information: Figure 1d–f). We then assessed whether furamidine modulates the methylation of KCNQ1 in cells. For this, HEK293T cells expressing Flag-tagged KCNQ1 (Flag-KCNQ1) and GFP-tagged KCNE1 (GFP-KCNE1) were incubated with 20 μM level of furamidine for 5 h. The cells were lysed and subjected to immunoprecipitation assay using anti-Flag antibodies. As shown in Figure 3d,e, the application of furamidine drastically decreased arginine monomethylation and asymmetric dimethylation of Flag-KCNQ1 without altering protein levels. Together, these data suggest the possibility that PRMT1 modulates I_{Ks} channel function by inducing arginine methylation of the KCNQ1 subunits of I_{Ks} channels.

3.4 | PRMT1 inhibition reduced I_{Ks} activities by decreasing its affinity for PIP_2

I_{Ks} channels require a certain level of PIP_2 in the cell membrane to maintain their activity (Park et al., 2005). PIP_2 binding to KCNQ1 subunits induces a large conformational change in the cytoplasmic domain and opening of the ion-conducting pathway through expansion of the S6 helices (Sun & MacKinnon, 2020). Because

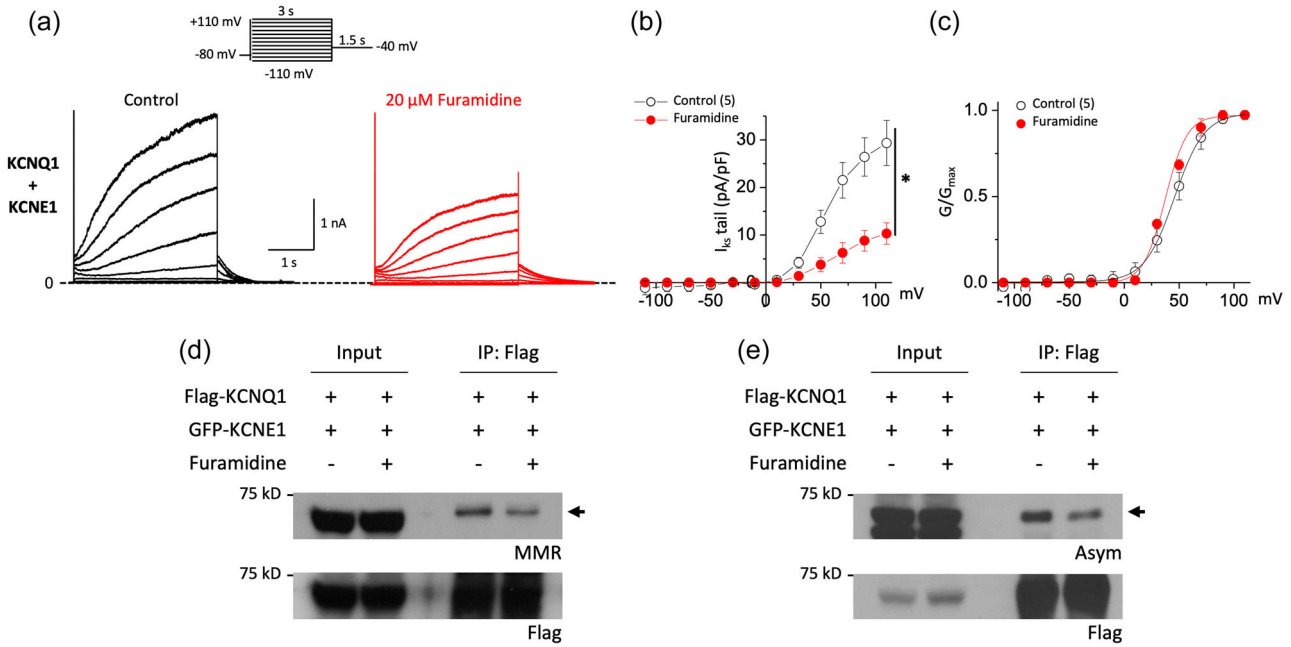

FIGURE 3 Furamidine induces a reduction in both I_{Ks} activity and KCNQ1 methylation in HEK 293T cells. (a) Representative current traces before (black) and after 20 μM furamidine treatment (red) from cells expressing human KCNQ1 and human KCNE1 channels. Cells were held at −80 mV, subjected to 3 s voltage steps ranging from −110 to +110 mV in 20 mV increments followed by a 1.5 s tail pulse at −40 mV (*inset*). (b) Tail current density–voltage relationship of I_{Ks} measured before (black) and after exposure to furamidine (red) showed the inhibitory effect of furamidine. (c) Voltage activation curves were obtained by plotting normalized tail currents versus the prepulse potential. Values for the midpoint of activation ($V_{1/2}$) were obtained by fitting with the Boltzmann equation (lines) as described in Section 2. (d,e) HEK293T cells were transfected with an equal amount of Flag-KCNQ1 and GFP-KCNE1 plasmids. Immunoprecipitation was performed using anti-Flag antibodies and monomethylation (MMR, d) or asymmetric dimethylation (ASYM, e) of the arginine residues of the precipitated proteins in the presence or absence of furamidine were analyzed by Western blotting. $^*p < 0.05$ by paired Student's *t*-test. All data are mean ± SEM. GFP, green fluorescent protein; IP, immunoprecipitation.

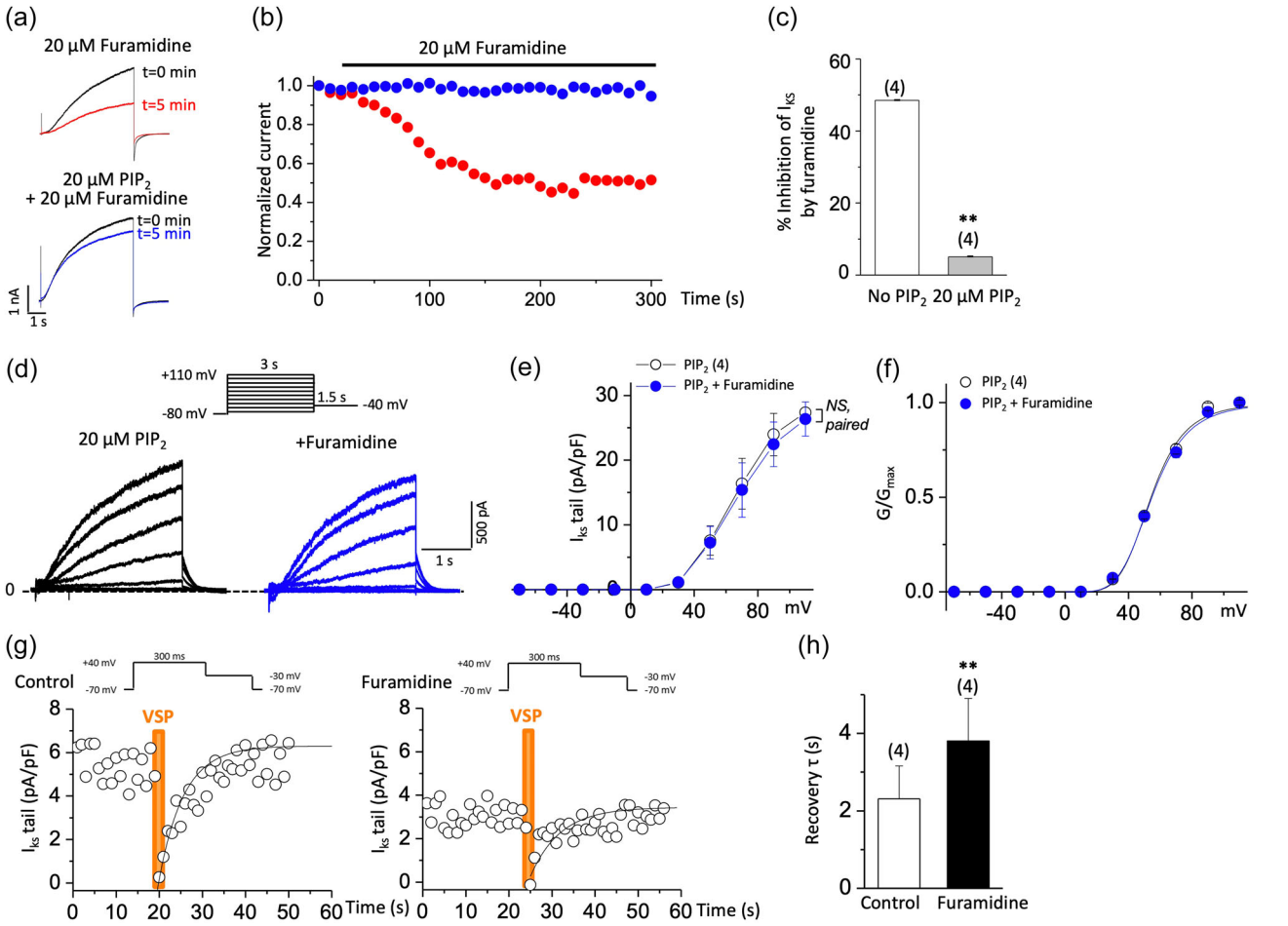

FIGURE 4 Furamidine decreases PIP_2 affinity of I_{Ks} channels. (a,b) Furamidine-induced inhibition of I_{Ks} and its prevention by diC8-PIP_2 in HEK293T cells. Current traces (a) and time course (b) show furamidine-induced inhibition of I_{Ks} (red circles). This inhibition was prevented by the addition of 20 μM diC8-PIP_2 in the patch pipette solution (blue circles). Currents were elicited by voltage steps from −80 to +80 mV for 5 s every 10 s and normalized to currents at $t = 0$. (c) Histogram depicting the extent of inhibition of I_{Ks} at +80 mV by furamidine treatment (20 μM, 5 min) in the absence or presence of 20 μM diC8-PIP_2 as indicated. $^{**}p < 0.01$ by Student's t-test. (d–f) Representative I_{Ks} traces evoked by depolarizing voltage steps as shown in the *inset* in HEK293T cells loaded with 20 μM diC8-PIP_2 (d), the corresponding I–V curves (e), and the corresponding voltage activation curves (f) before (black) and after 20 μM furamidine treatment (blue). NS, not significantly different; paired Student's t-test. (g,h) Quantitative determination of the sensitivity of I_{Ks} to activation of Dr-VSP in HEK293T cells transfected with Dr-VSP and human KCNQ1 + human KCNE1. Tail current amplitudes were used to measure current inhibition by Dr-VSP activation and its recovery. Time course of I_{Ks} tail before (left) and after 20 μM furamidine treatment (right) (g). Data were fitted with a single exponential (smooth curves). The time constant (τ) of an exponential fit of recovery before and after 20 μM furamidine treatment (h). Membrane was held at −70 mV and depolarized to +40 mV for 300 ms every 1 s, except for the shaded area in orange where the membrane was held at +100 mV for 2 s (*inset*). Tail currents were measured during slow channel deactivation at −30 mV. $^{**}p < 0.01$ by paired Student's t-test. Dr-VSP, voltage-sensitive phosphatase from *Danio rerio*;PIP_2, phosphatidylinositol 4,5-bisphosphate.

arginine methylation increases KCNQ2 channel-PIP_2 interactions (Kim et al., 2016), we reasoned that PRMT1 inhibition might reduce I_{Ks} channel activities by decreasing the PIP_2 binding affinity of the KCNQ1 subunits. To test this, we investigated whether exogenous PIP_2 loading blocked furamidine-induced I_{Ks} inhibition. We included 20 μM of the water-soluble PIP_2 analog, diC8-PIP_2, in the patch pipette solution and tested the furamidine effects after rupturing the plasma membrane. Adding 20 μM diC8-PIP_2 to the patch pipette solution prevented furamidine-induced inhibition of the I_{Ks} activities in HEK293T cells (Figure 4a,b). The extents of the I_{Ks} inhibition with and without 20 μM diC8-PIP_2 were 48.5 ± 0.1% ($n = 4$) and 5.05 ± 0.13% ($n = 4$, $p < 0.01$), respectively (Figure 4c). Additional experiments confirmed that both the time-dependent currents elicited by 3-s depolarizations and the tail currents during the subsequent repolarization to −40 mV became insensitive to furamidine owing to the 20 μM diC8-PIP_2 (Figure 4d–f; $n = 4$), suggesting that furamidine treatment reduces I_{Ks} by modulating PIP_2 affinity.

The altered PIP_2 affinity induced by furamidine was also assessed via a Dr-VSP, which hydrolyzes PIP_2 at highly depolarized voltages (e.g., +100 mV) and transiently reduces PIP_2 levels (Falkenburger et al., 2010; Kim et al., 2016). Dr-VSP was coexpressed with human KCNQ1 and KCNE1, and its activity was elicited by membrane

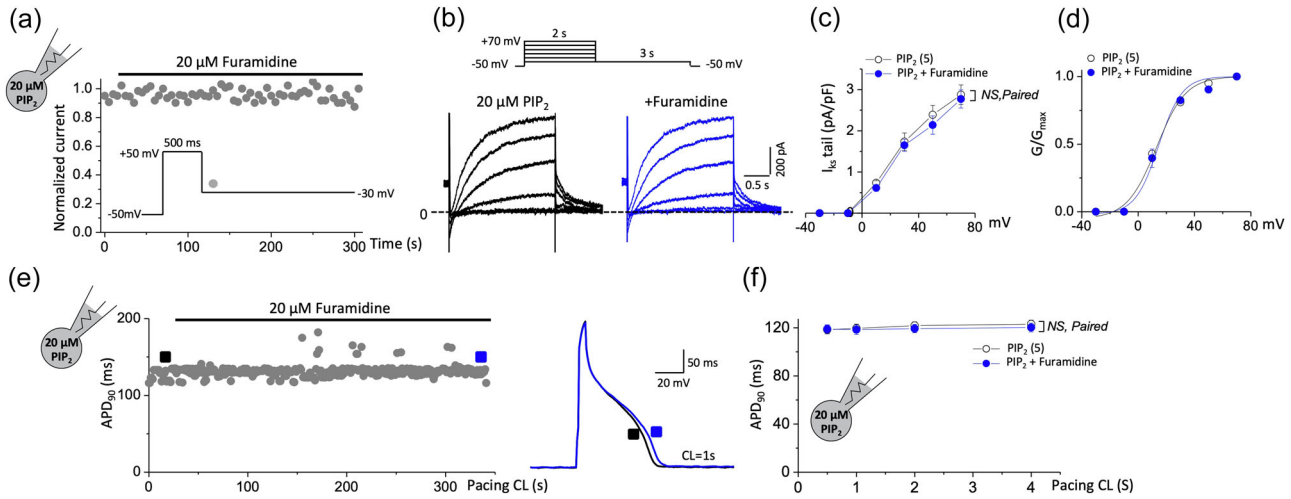

FIGURE 5 PIP_2 prevented furamidine-induced I_{Ks} reduction and APD prolongation in cardiomyocytes. (a) The time course of I_{Ks} tail of guinea pig ventricular myocytes shows that the inhibition I_{Ks} by furamidine was almost completely blocked when loaded with 20 μM diC8-PIP_2. Currents were elicited by a voltage step to +50 mV at a holding potential of −50 mV with a subsequent step to −30 mV for the tail current (*inset*). (b–d) Representative I_{Ks} traces evoked by depolarizing voltage steps as shown in the *inset* in guinea pig ventricular myocytes loaded with 20 μM diC8-PIP_2 (b), the corresponding *I*–*V* curves (c), and the corresponding voltage activation curves (d) before (black) and after 20 μM furamidine treatment (blue). (e) The time course of APD_{90} in a guinea pig ventricular myocyte with 20 μM diC8-PIP_2 in the recording pipette in response to 20 μM furamidine. Right, representative AP trace before (black) and after (blue) 20 μM furamidine treatment from left. (f) The summary data for the APD_{90} from guinea pig ventricular myocytes during stimulation at various pacing CL with 20 μM diC8-PIP_2 in the patch pipette before (black) and after 20 μM furamidine treatment (blue). NS, not significantly different versus furamidine treatment; paired Student's *t*-test. All data are mean ± SEM. APD, action potential duration; APD_{90}, APD at 90% repolarization; CL, cycle length; PIP_2, phosphatidylinositol 4,5-bisphosphate.

depolarization. Consistent with the previous report (Li et al., 2011), Dr-VSP activation reduced the I_{Ks}, and the currents were recovered quickly after PIP_2 resynthesis on repolarization (Figure 4g, left). Subjecting I_{Ks} to the same VSP activation protocol following 20 μM furamidine treatment further reduced the currents and slowed their recovery (Figure 4g, right). The mean recovery time constant of I_{Ks} tail was increased by twofold after furamidine treatment ($p < 0.01$; Figure 4h). The slowed recovery after Dr-VSP activation reflected the reduced PIP_2 affinity (Falkenburger et al., 2010), further supporting that furamidine reduced the PIP_2 affinity of the I_{Ks} channels.

3.5 | Adding PIP_2 to cardiomyocytes prevented furamidine-induced I_{Ks} reduction and APD prolongation

We then tested whether adding exogenous PIP_2 could prevent the effects of furamidine on I_{Ks} in guinea pig ventricular myocytes. While the 20 μM furamidine-induced inhibition of the I_{Ks} tail started within 10 s and gradually reached a steady-state level within 5 min (Figure 2b), furamidine application to guinea pig ventricular myocytes in the presence of 20 μM diC8-PIP_2 in the patch pipette solution did not affect the I_{Ks} tail after 5 min (Figure 5a). Figure 5b shows the representative traces of the I_{Ks} recorded in ventricular myocytes loaded with 20 μM diC8-PIP_2, evoked by 2-s depolarizing voltage steps from −30 to +70 mV, each of which was followed by a repolarizing step, before and after 5 min of furamidine treatment. The developing currents observed during the depolarization steps and the tail currents observed on the return to −30 mV were once again unaffected by furamidine treatment. The *I*–*V* curves of the I_{Ks} tail and the steady-state activation curves before (black) and after (blue) furamidine treatment showed that adding exogenous PIP_2 blocked the furamidine-induced inhibition of ventricular I_{Ks} (Figure 5c,d). Furthermore, 20 μM diC8-PIP_2 did not affect the control I_{Ks} currents (tail currents at +70 mV in the presence of PIP_2: 2.77 ± 0.22 pA/pF, $p > 0.05$ vs. 2.87 ± 0.23 pA/pF without PIP_2), suggesting that the PIP_2 concentration in the membrane was not a limiting factor for I_{Ks} activation under normal conditions. Because PIP_2 prevented furamidine-induced I_{Ks} inhibition, we assessed whether PIP_2 could also prevent furamidine-induced APD prolongation in ventricular myocytes. Figure 5e shows representative ventricular APs, illustrating that, in the presence of 20 μM diC8-PIP_2, AP at one CL remained unchanged upon application of 20 μM furamidine. APD_{90} before and after furamidine treatment did not significantly differ at any CL, indicating that adding exogenous PIP_2 blocked furamidine-mediated cardiac APD prolongation (Figure 5f). These results suggest that adding PIP_2 prevented furamidine from inducing a reduction of I_{Ks} function. Thus, PRMT1 inhibition reduced the affinity between the KCNQ1/KCNE1 channel complex and PIP_2, thus reducing the I_{Ks} and prolonging APD.

4 | DISCUSSION

Here, we demonstrate that PRMT1 positively regulates I_{Ks} channel activity, thereby restricting excess cardiac AP. In guinea pig ventricular myocytes, a specific inhibitor of PRMT1, furamidine, prolongs ventricular APD, mainly via I_{Ks}. PRMT1 inhibition decreases

the I_{Ks} channel activity formed by heterologous expression of KCNQ1 and KCNE1 subunits in HEK293T cells as well as I_{Ks} in cardiac myocytes and this coincides with a marked reduction in arginine monomethylation of KCNQ1 subunits. We provide evidence that PRMT1 regulates I_{Ks} activity via modulation of PIP_2 affinity of I_{Ks} channels in HEK293T cells. Consistently, applying exogenous PIP_2 to cardiomyocytes prevents furamidine-induced I_{Ks} reduction and APD prolongation. These findings suggest that PRMT1 is an important regulator of I_{Ks} channel activity and thus of cardiac repolarization.

In ventricular AP, I_{Ks} is a major contributor to the ventricular "repolarization reserve" by providing redundant current to maintain rapid repolarization during increases in the cardiac rate or during conditions in which other ventricular potassium currents are reduced (e.g., pharmacological inhibition of I_{Kr}) (Roden, 2006). Accordingly, I_{Ks} reduction results in APD prolongation and the development of potentially fatal ventricular arrhythmias, particularly during sustained adrenergic tone or heart failure where I_{Kr} is also reduced, making the contributions of I_{Ks} to repolarization in the ventricle more critical (Shugg et al., 2020). Various molecular mechanisms for I_{Ks} reduction in heart failure have been proposed and sustained activation of the sympathetic nervous system and renin–angiotensin–aldosterone system (RAAS) signaling pathways are suggested to be key mediators of I_{Ks} pathophysiology (Shugg et al., 2020). In contrast to acute β-adrenergic receptor stimulation-induced increase in I_{Ks}, sustained β-adrenergic receptor stimulation has been demonstrated to reduce I_{Ks} through two distinct pathways: the first involving activation of the exchange protein activated by cAMP and the second involving activation of calcium/calmodulin-dependent protein kinase II (CaMKII) (Aflaki et al., 2014; Shugg et al., 2018). Sustained elevations in RAAS signaling, mediated largely through activation of the angiotensin II type 1 receptor (AT1) by angiotensin II, have also been demonstrated to affect I_{Ks}. Sustained treatment with angiotensin II reduces I_{Ks} through a mechanism involving cellular depletion of PIP_2 in response to Gq-coupled AT1 signaling (Matavel & Lopes, 2009). Our data identify the role of PRMT1 signaling in regulating the PIP_2 affinity of I_{Ks} in cardiac myocytes. The regulatory role of PRMT1 on I_{Ks} may be of significance in heart failure since past investigations have found that PRMT1 is downregulated in heart failure (Pyun et al., 2018). The downregulated or deregulated PRMT1 activity may lead to reductions in I_{Ks} activity via decreases in PIP_2 affinity of I_{Ks} channels. Thus, the effects of PRMT1 downregulation and sustained neurohormonal signaling may converge on the reduction of I_{Ks} channel–PIP_2 interaction in heart failure. Further research is needed to explore this possibility.

Posttranslational modifications of the KCNQ1–KCNE1 channel complex are known to be vital for regulating the cardiac I_{Ks} current. Sumoylation, phosphorylation, and *O*-glycosylation regulate I_{Ks} channels, each of which is essential for I_{Ks} functions such as voltage-dependent channel activation, β-adrenergic signaling, and anterograde trafficking (Chandrasekhar et al., 2011; Marx et al., 2002; Xiong et al., 2017). Our data suggest that PRMT1-specific inhibition reduced arginine methylation of the KCNQ1 subunits, and the methylation level correlated with I_{Ks} activities. Positively charged (basic) arginine, histidine, and lysine residues are candidates for mediating electrostatic interaction with PIP_2 in channels such as KCNQ (Hernandez et al., 2008), Kir2 (Hansen et al., 2011; C. L. Huang et al., 1998; Lopes et al., 2002), G protein-gated inwardly rectifying potassium (Whorton & MacKinnon, 2011), and HERG (J.-S. Bian et al., 2004). Because each additional methyl group to an arginine residue can stabilize the positive charge of the residue in proteins under physiological conditions and likely facilitate their electrostatic interactions with negatively charged molecules (Bedford & Clarke, 2009; Shearer, 2008), methylation of arginine residues in KCNQ1 may promote electrostatic binding of KCNQ1 to PIP_2 and thus channel activity. Like I_{Ks} channels, HERG/I_{Kr} channels, one of the K^+ channels that regulate the rate of AP repolarization, are regulated by PIP_2 signaling in cardiac myocytes (J.-S. Bian et al., 2004). It was shown that stimulation of α1-adrenergic receptors reduces HERG channel activity as well as I_{Ks} via PIP_2 depletion (J. Bian et al., 2001). However, HERG/I_{Kr} channel was not significantly associated with the furamidine-induced APD prolongation in this study (Figure 1). Thus, it appears that PRMT1 does not regulate all PIP_2-dependent channels, but its effects are specific to the selected target ion channels. This is consistent with previous findings that PRMT1 specifically regulates KCNQ2/KCNQ3 channels in hippocampal dentate granule cells, while leak-channel NALCN in the same cells is methylated and regulated by PRMT7 (Kim et al., 2016; Lee et al., 2019).

Our data indicate that PRMT1 is required for the I_{Ks} channel activity to ensure normal cardiac AP. Along with the results of a previous study showing that PRMT1 prevents contractile dysfunction and heart failure by inhibiting cardiac CaMKII hyperactivation (Pyun et al., 2018), our data suggest that PRMT1 activity loss simultaneously affects the mechanical and electrical properties of heart muscle cells. In addition, it is possible that the proarrhythmogenic potential of reductions in I_{Ks} is further enhanced during sustained CaMKII activation in response to PRMT1 downregulation since CaMKII hyperactivation results in alterations in a wide variety of ion channels and Ca^{2+} handling proteins, including ryanodine receptor, and sarco/endoplasmic reticulum Ca^{2+}-ATPase (Swaminathan et al., 2012). Although heart failure is a mechanical problem, mostly of contraction (inotropy) but also relaxation (lusitropy), many patients with heart failure experience arrhythmias, which are electrical problems. Despite the clear association between heart failure and arrhythmias, widely applicable treatments to simultaneously treat both diseases have been difficult to develop. Rather than targeting and modulating the ion channels themselves, targeting the post-translational modifications of ion channels, which have more subtle effects on excitability, might prove to be an interesting alternative to treat arrhythmias (Galleano et al., 2021). Therefore, the benefits of PRMT1 on CaMKII and I_{Ks} in cardiomyocytes open the possibility of using the PRMT1 signaling pathway as a novel therapeutic target for treating both heart failure and arrhythmias.

ACKNOWLEDGMENTS

This study was supported by the National Research Foundation of Korea Grants NRF-2020R1A2C2012846 awarded to Hana Cho and NRF-2019R1A2C2003767 awarded to Ilmin Kwon.

CONFLICTS OF INTEREST

The authors declare no conflicts of interest.

ORCID

Hana Cho http://orcid.org/0000-0002-9394-8671

REFERENCES

Aflaki, M., Qi, X. Y., Xiao, L., Ordog, B., Tadevosyan, A., Luo, X., Maguy, A., Shi, Y., Tardif, J. C., & Nattel, S. (2014). Exchange protein directly activated by cAMP mediates slow delayed-rectifier current remodeling by sustained β-adrenergic activation in guinea pig hearts. *Circulation Research*, *114*(6), 993–1003. https://doi.org/10.1161/circresaha.113.302982

Albrecht, L. V., Zhang, L., Shabanowitz, J., Purevjav, E., Towbin, J. A., Hunt, D. F., & Green, K. J. (2015). GSK3- and PRMT-1-dependent modifications of desmoplakin control desmoplakin–cytoskeleton dynamics. *Journal of Cell Biology*, *208*(5), 597–612. https://doi.org/10.1083/jcb.201406020

Bedford, M. T., & Clarke, S. G. (2009). Protein arginine methylation in mammals: Who, what, and why. *Molecular Cell*, *33*(1), 1–13. https://doi.org/10.1016/j.molcel.2008.12.013

Bedford, M. T., & Richard, S. (2005). Arginine methylation an emerging regulator of protein function. *Molecular Cell*, *18*(3), 263–272. https://doi.org/10.1016/j.molcel.2005.04.003

Bian, J., Cui, J., & McDonald, T. V. (2001). HERG K(+) channel activity is regulated by changes in phosphatidyl inositol 4,5-bisphosphate. *Circulation Research*, *89*(12), 1168–1176. https://doi.org/10.1161/hh2401.101375

Bian, J.-S., Kagan, A., & McDonald, T. V. (2004). Molecular analysis of PIP2 regulation of HERG and I_{kr}. *American Journal of Physiology: Heart and Circulatory Physiology*, *287*(5), H2154–H2163. https://doi.org/10.1152/ajpheart.00120.2004

Biggar, K. K., & Li, S. S. (2015). Non-histone protein methylation as a regulator of cellular signalling and function. *Nature Reviews Molecular Cell Biology*, *16*(1), 5–17. https://doi.org/10.1038/nrm3915

Blanc, R. S., Vogel, G., Li, X., Yu, Z., Li, S., & Richard, S. (2017). Arginine methylation by PRMT1 regulates muscle stem cell fate. *Molecular and Cellular Biology*, *37*(3):e00457. https://doi.org/10.1128/mcb.00457-16

Bosch, R. F., Gaspo, R., Busch, A. E., Lang, H. J., Li, G. R., & Nattel, S. (1998). Effects of the chromanol 293B, a selective blocker of the slow, component of the delayed rectifier K+ current, on repolarization in human and guinea pig ventricular myocytes. *Cardiovascular Research*, *38*(2), 441–450. https://doi.org/10.1016/s0008-6363(98)00021-2

Cardiac Arrhythmia Suppression Trial Investigators. (1989). Preliminary report: Effect of encainide and flecainide on mortality in a randomized trial of arrhythmia suppression after myocardial infarction. *New England Journal of Medicine*, *321*(6), 406–412. https://doi.org/10.1056/nejm198908103210629

Chandrasekhar, K. D., Lvov, A., Terrenoire, C., Gao, G. Y., Kass, R. S., & Kobertz, W. R. (2011). O-glycosylation of the cardiac I(Ks) complex. *Journal of Physiology*, *589*(Pt 15), 3721–3730. https://doi.org/10.1113/jphysiol.2011.211284

Choi, S. H., Lee, B. H., Kim, H. J., Jung, S. W., Kim, H. S., Shin, H. C., Lee, J. H., Kim, H. C., Rhim, H., Hwang, S. H., Ha, T. S., Kim, H. J., Cho, H., & Nah, S. Y. (2014). Ginseng gintonin activates the human cardiac delayed rectifier K+ channel: Involvement of Ca2+/calmodulin binding sites. *Molecules and Cells*, *37*(9), 656–663. https://doi.org/10.14348/molcells.2014.0087

Choi, D., Oh, K. J., Han, H. S., Yoon, Y. S., Jung, C. Y., Kim, S. T., & Koo, S. H. (2012). Protein arginine methyltransferase 1 regulates hepatic glucose production in a FoxO1-dependent manner. *Hepatology*, *56*(4), 1546–1556. https://doi.org/10.1002/hep.25809

Delmas, P., & Brown, D. A. (2005). Pathways modulating neural KCNQ/M (Kv7) potassium channels. *Nature Reviews Neuroscience*, *6*(11), 850–862. https://doi.org/10.1038/nrn1785

Di Lorenzo, A., & Bedford, M. T. (2011). Histone arginine methylation. *FEBS Letters*, *585*(13), 2024–2031. https://doi.org/10.1016/j.febslet.2010.11.010

Eram, M. S., Shen, Y., Szewczyk, M., Wu, H., Senisterra, G., Li, F., Butler, K. V., Kaniskan, H., Speed, B. A., Dela Seña, C., Dong, A., Zeng, H., Schapira, M., Brown, P. J., Arrowsmith, C. H., Barsyte-Lovejoy, D., Liu, J., Vedadi, M., & Jin, J. (2016). A potent, selective, and cell-active inhibitor of human type I protein arginine methyltransferases. *ACS Chemical Biology*, *11*(3), 772–781. https://doi.org/10.1021/acschembio.5b00839

Falkenburger, B. H., Jensen, J. B., & Hille, B. (2010). Kinetics of PIP2 metabolism and KCNQ2/3 channel regulation studied with a voltage-sensitive phosphatase in living cells. *Journal of General Physiology*, *135*(2), 99–114. https://doi.org/10.1085/jgp.200910345

Fedoriw, A., Rajapurkar, S. R., O'Brien, S., Gerhart, S. V., Mitchell, L. H., Adams, N. D., Rioux, N., Lingaraj, T., Ribich, S. A., Pappalardi, M. B., Shah, N., Laraio, J., Liu, Y., Butticello, M., Carpenter, C. L., Creasy, C., Korenchuk, S., McCabe, M. T., McHugh, C. F., … Mohammad, H. P. (2019). Anti-tumor activity of the type I PRMT Inhibitor, GSK3368715, synergizes with PRMT5 Inhibition through MTAP loss. *Cancer Cell*, *36*(1), 100–114.e125. https://doi.org/10.1016/j.ccell.2019.05.014

Galleano, I., Harms, H., Choudhury, K., Khoo, K., Delemotte, L., & Pless, S. A. (2021). Functional cross-talk between phosphorylation and disease-causing mutations in the cardiac sodium channel Nav1.5. *Proceedings of the National Academy of Sciences of the United States of America*, *118*(33), e2025320118. https://doi.org/10.1073/pnas.2025320118

Hansen, S. B., Tao, X., & MacKinnon, R. (2011). Structural basis of PIP2 activation of the classical inward rectifier K+ channel Kir2.2. *Nature*, *477*(7365), 495–498. https://doi.org/10.1038/nature10370

Hernandez, C. C., Zaika, O., & Shapiro, M. S. (2008). A carboxy-terminal inter-helix linker as the site of phosphatidylinositol 4,5-bisphosphate action on Kv7 (M-type) K+ channels. *Journal of General Physiology*, *132*(3), 361–381. https://doi.org/10.1085/jgp.200810007

Huang, C. L., Feng, S., & Hilgemann, D. W. (1998). Direct activation of inward rectifier potassium channels by PIP2 and its stabilization by Gbetagamma. *Nature*, *391*(6669), 803–806. https://doi.org/10.1038/35882

Huang, S., Litt, M., & Felsenfeld, G. (2005). Methylation of histone H4 by arginine methyltransferase PRMT1 is essential in vivo for many subsequent histone modifications. *Genes and Development*, *19*(16), 1885–1893. https://doi.org/10.1101/gad.1333905

Ki, C. S., Jung, C. L., Kim, H. J., Baek, K. H., Park, S. J., On, Y. K., Kim, K. S., Noh, S. J., Youm, J. B., Kim, J. S., & Cho, H. (2014). A KCNQ1 mutation causes age-dependant bradycardia and persistent atrial fibrillation. *Pflugers Archiv: European Journal of Physiology*, *466*(3), 529–540. https://doi.org/10.1007/s00424-013-1337-6

Kienitz, M. C., Vladimirova, D., Müller, C., Pott, L., & Rinne, A. (2016). Receptor species-dependent desensitization controls KCNQ1/KCNE1 K+ channels as downstream effectors of Gq protein-coupled receptors. *Journal of Biological Chemistry*, *291*(51), 26410–26426. https://doi.org/10.1074/jbc.M116.746974

Kim, H. J., Jeong, M. H., Kim, K. R., Jung, C. Y., Lee, S. Y., Kim, H., Koh, J., Vuong, T. A., Jung, S., Yang, H., Park, S. K., Choi, D., Kim, S. H., Kang, K., Sohn, J. W., Park, J. M., Jeon, D., Koo, S. H., Ho, W. K., … Cho, H. (2016). Protein arginine methylation facilitates KCNQ channel-PIP2 interaction leading to seizure suppression. *Elife*, *5*, e17159. https://doi.org/10.7554/eLife.17159

Lee, S. Y., Vuong, T. A., Wen, X., Jeong, H. J., So, H. K., Kwon, I., Kang, J. S., & Cho, H. (2019). Methylation determines the extracellular calcium

sensitivity of the leak channel NALCN in hippocampal dentate granule cells. *Experimental & Molecular Medicine*, *51*(10), 1–14. https://doi.org/10.1038/s12276-019-0325-0

Li, Y., Zaydman, M. A., Wu, D., Shi, J., Guan, M., Virgin-Downey, B., & Cui, J. (2011). KCNE1 enhances phosphatidylinositol 4,5-bisphosphate (PIP2) sensitivity of I_{ks} to modulate channel activity. *Proceedings of the National Academy of Sciences of the United States of America*, *108*(22), 9095–9100. https://doi.org/10.1073/pnas.1100872108

Liu, Z., Du, L., & Li, M. (2012). Update on the slow delayed rectifier potassium current (I_{ks}): Role in modulating cardiac function. *Current Medicinal Chemistry*, *19*(9), 1405–1420. https://doi.org/10.2174/092986712799462595

Lo, C. F., & Numann, R. (1998). Independent and exclusive modulation of cardiac delayed rectifying K+ current by protein kinase C and protein kinase A. *Circulation Research*, *83*(10), 995–1002. https://doi.org/10.1161/01.res.83.10.995

Lopes, C. M., Zhang, H., Rohacs, T., Jin, T., Yang, J., & Logothetis, D. E. (2002). Alterations in conserved Kir channel-PIP2 interactions underlie channelopathies. *Neuron*, *34*(6), 933–944. https://doi.org/10.1016/s0896-6273(02)00725-0

Marx, S. O., Kurokawa, J., Reiken, S., Motoike, H., D'Armiento, J., Marks, A. R., & Kass, R. S. (2002). Requirement of a macromolecular signaling complex for beta adrenergic receptor modulation of the KCNQ1-KCNE1 potassium channel. *Science*, *295*(5554), 496–499. https://doi.org/10.1126/science.1066843

Matavel, A., & Lopes, C. M. (2009). PKC activation and PIP(2) depletion underlie biphasic regulation of I_{ks} by Gq-coupled receptors. *Journal of Molecular and Cellular Cardiology*, *46*(5), 704–712. https://doi.org/10.1016/j.yjmcc.2009.02.006

Matavel, A., Medei, E., & Lopes, C. M. (2010). PKA and PKC partially rescue long QT type 1 phenotype by restoring channel-PIP2 interactions. *Channels*, *4*(1), 3–11. https://doi.org/10.4161/chan.4.1.10227

Murata, K., Lu, W., Hashimoto, M., Ono, N., Muratani, M., Nishikata, K., Kim, J. D., Ebihara, S., Ishida, J., & Fukamizu, A. (2018). PRMT1 deficiency in mouse juvenile heart induces dilated cardiomyopathy and reveals cryptic alternative splicing products. *iScience*, *8*, 200–213. https://doi.org/10.1016/j.isci.2018.09.023

Nuss, H. B., & Marban, E. (1994). Electrophysiological properties of neonatal mouse cardiac myocytes in primary culture. *Journal of Physiology*, *479*(Pt 2Pt 2), 265–279. https://doi.org/10.1113/jphysiol.1994.sp020294

Park, K. H., Piron, J., Dahimene, S., Mérot, J., Baró, I., Escande, D., & Loussouarn, G. (2005). Impaired KCNQ1-KCNE1 and phosphatidylinositol-4,5-bisphosphate interaction underlies the long QT syndrome. *Circulation Research*, *96*(7), 730–739. https://doi.org/10.1161/01.RES.0000161451.04649.a8

Pyun, J. H., Kim, H. J., Jeong, M. H., Ahn, B. Y., Vuong, T. A., Lee, D. I., Choi, S., Koo, S. H., Cho, H., & Kang, J. S. (2018). Cardiac specific PRMT1 ablation causes heart failure through CaMKII dysregulation. *Nature Communications*, *9*(1), 5107. https://doi.org/10.1038/s41467-018-07606-y

Roden, D. M. (2006). Long QT syndrome: Reduced repolarization reserve and the genetic link. *Journal of Internal Medicine*, *259*(1), 59–69. https://doi.org/10.1111/j.1365-2796.2005.01589.x

Schumacher, S. M., & Martens, J. R. (2010). Ion channel trafficking: A new therapeutic horizon for atrial fibrillation. *Heart Rhythm*, *7*(9), 1309–1315. https://doi.org/10.1016/j.hrthm.2010.02.017

Shearer, J. (2008). Influence of sequential guanidinium methylation on the energetics of the guanidinium···guanine dimer and guanidinium···guanine···cytosine trimer: Implications for the control of protein···DNA interactions by arginine methyltransferases. *The Journal of Physical Chemistry B*, *112*(51), 16995–17002. https://doi.org/10.1021/jp808288p

Shugg, T., Hudmon, A., & Overholser, B. R. (2020). Neurohormonal regulation of I(Ks) in heart failure: Implications for ventricular arrhythmogenesis and sudden cardiac death. *Journal of the American Heart Association*, *9*(18), e016900. https://doi.org/10.1161/jaha.120.016900

Shugg, T., Johnson, D. E., Shao, M., Lai, X., Witzmann, F., Cummins, T. R., Rubart-Von-der Lohe, M., Hudmon, A., & Overholser, B. R. (2018). Calcium/calmodulin-dependent protein kinase II regulation of I(Ks) during sustained β-adrenergic receptor stimulation. *Heart Rhythm*, *15*(6), 895–904. https://doi.org/10.1016/j.hrthm.2018.01.024

Sun, J., & MacKinnon, R. (2020). Structural basis of human KCNQ1 modulation and gating. *Cell*, *180*(2), 340–347.e349. https://doi.org/10.1016/j.cell.2019.12.003

Swaminathan, P. D., Purohit, A., Hund, T. J., & Anderson, M. E. (2012). Calmodulin-dependent protein kinase II: Linking heart failure and arrhythmias. *Circulation Research*, *110*(12), 1661–1677. https://doi.org/10.1161/circresaha.111.243956

Tobelaim, W. S., Dvir, M., Lebel, G., Cui, M., Buki, T., Peretz, A., Marom, M., Haitin, Y., Logothetis, D. E., Hirsch, J. A., & Attali, B. (2017). Ca(2+)-calmodulin and PIP2 interactions at the proximal C-terminus of Kv7. *Channels*, *11*(6), 686–695. https://doi.org/10.1080/19336950.2017.1388478

Waldo, A. L., Camm, A. J., deRuyter, H., Friedman, P. L., MacNeil, D. J., Pauls, J. F., Pitt, B., Pratt, C. M., Schwartz, P. J., & Veltri, E. P., The SWORD Investigators. (1996). Effect of D-sotalol on mortality in patients with left ventricular dysfunction after recent and remote myocardial infarction. *Lancet*, *348*(9019), 7–12. https://doi.org/10.1016/s0140-6736(96)02149-6

Wang, K., Terrenoire, C., Sampson, K. J., Iyer, V., Osteen, J. D., Lu, J., Keller, G., Kotton, D. N., & Kass, R. S. (2011). Biophysical properties of slow potassium channels in human embryonic stem cell derived cardiomyocytes implicate subunit stoichiometry. *Journal of Physiology*, *589*(Pt 24), 6093–6104. https://doi.org/10.1113/jphysiol.2011.220863

Whorton, M. R., & MacKinnon, R. (2011). Crystal structure of the mammalian GIRK2 K+ channel and gating regulation by G proteins, PIP2, and sodium. *Cell*, *147*(1), 199–208. https://doi.org/10.1016/j.cell.2011.07.046

Xiong, D., Li, T., Dai, H., Arena, A. F., Plant, L. D., & Goldstein, S. A. N. (2017). SUMOylation determines the voltage required to activate cardiac I(Ks) channels. *Proceedings of the National Academy of Sciences of the United States of America*, *114*(32), E6686–e6694. https://doi.org/10.1073/pnas.1706267114

Zhang, Y., Verwilligen, R. A. F., de Boer, M., Sijsenaar, T. J. P., Van Eck, M., & Hoekstra, M. (2021). PRMT4 inhibitor TP-064 impacts both inflammatory and metabolic processes without changing the susceptibility for early atherosclerotic lesions in male apolipoprotein E knockout mice. *Atherosclerosis*, *338*, 23–29. https://doi.org/10.1016/j.atherosclerosis.2021.11.001

SUPPORTING INFORMATION

Additional supporting information can be found online in the Supporting Information section at the end of this article.

How to cite this article: An, X., Lee, J., Kim, G. H., Kim, H.-J., Pyo, H.-J., Kwon, I., & Cho, H. (2022). Modulation of I_{Ks} channel–PIP_2 interaction by PRMT1 plays a critical role in the control of cardiac repolarization. *Journal of Cellular Physiology*, 237, 3069–3079. https://doi.org/10.1002/jcp.30775